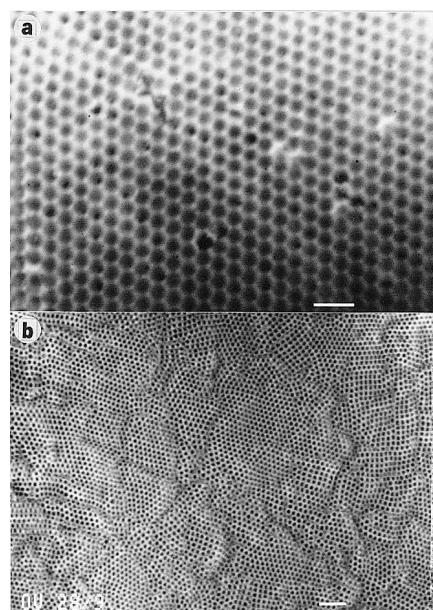


**Figure 1** Micrographs of ordered latex templates. **a**, Optical microscopy in transmitted light. The different colours probably correspond to crystal domains of different symmetry or orientation. **b**, Scanning electron micrograph (SEM). Ordered latex layers display either hexagonal or cubic packing. Scale bars: 50  $\mu\text{m}$  and 1  $\mu\text{m}$ , respectively.

media. The latex particles accumulated slowly on the membrane surface, building up closely packed, ordered layers roughly 10  $\mu\text{m}$  thick. The deposited crystalline layer could be broken and detached from the membrane surface for analysis by light and scanning electron microscopy (Fig. 1).

To induce silica polymerization the microsphere surfaces had to be functionalized *in situ* by adsorption of the surfactant hexadecyltrimethyl ammonium bromide (HTAB). We soaked the crystalline latex layers with 0.02 M HTAB solution for 20 min, then removed the excess unadsorbed surfactant by washing briefly with deionized water. We mineralized the cavities in the arrays by passing 0.5 M silica solution through the latex-covered filter. The permeability of the layers decreased as the polymerization process continued, so that flow through the filter stopped in less than one minute. When the silica solution had gelled inside the colloidal crystal layer, we removed the excess solution and dried the latex/silica composite under vacuum. The latex templates inside the polymerized silica were removed by heating at 450  $^{\circ}\text{C}$  for 4 h, leaving silica flakes of very low density as the final product.

Scanning electron microscopy shows that the material is built up of three-dimensional ordered arrays of uniform pores. Examples of the discrete morphology of the material are shown in Fig. 2. By varying the size of the latex microspheres used, we were able to produce organized materials with pore sizes ranging from about 150 nm to



**Figure 2** SEM of the microporous silica structures. Latex particles of **a**, 560 nm and **b**, 300 nm diameters were used as templates. Large ordered arrays of spherical cavities, representing a negative replica of the original colloidal crystal embedded in the silica, are seen. The silica flakes appear to be built up of many similar domains with different crystal orientations. Details of materials and methods are available on request from the authors. Scale bars, 1  $\mu\text{m}$ .

1  $\mu\text{m}$ . A comparison between the repeat units of the silica replicas and the original latex crystals showed that the baked materials had shrunk by 20–35%, a value that is higher than, but comparable to, that in the M41S mesoporous silicas<sup>1</sup>.

Our results show that it is possible to obtain highly structured silica materials in which the pore size, shape and ordering can be precisely controlled within a wide range that has previously been unattainable. The method is powerful and controllable, and could be adapted for large-scale production.

**O. D. Velev, T. A. Jede  
R. F. Lobo, A. M. Lenhoff**

Department of Chemical Engineering,  
University of Delaware, Newark,  
Delaware 19716, USA  
e-mail: velev@che.udel.edu

1. Kresge, C. T., Leonowicz, M. E., Roth, W. J., Vartuli, J. C. & Beck, J. S. *Nature* **359**, 710–712 (1992).
2. Beck, J. S. *et al.* *J. Am. Chem. Soc.* **114**, 10834–10843 (1992).
3. Monnier, A. *et al.* *Science* **261**, 1299–1303 (1993).
4. Raman, K. N., Anderson, M. T. & Brinker, C. J. *Chem. Mater.* **8**, 1682–1701 (1996).
5. Davis, S. A., Burkett, S. L., Mendelson, N. H. & Mann, S. *Nature* **385**, 420–423 (1997).
6. Mann, S. & Ozin, G. A. *Nature* **382**, 313–318 (1996).
7. Arora, A. K. & Rajagopalan, R. in *Ordering and Phase Transitions in Charged Colloids* (eds Arora, A. K. & Tata, B. V. R.) 1–13 (VCH, New York, 1996).
8. Larsen, A. E. & Grier, D. G. *Nature* **385**, 230–233 (1997).
9. Trau, M., Saville, D. A. & Aksay, I. A. *Science* **272**, 706–709 (1996).
10. Denkov, N. D. *et al.* *Nature* **361**, 26 (1993).
11. van Blaaderen, A., Ruel, R. & Wiltzius, P. *Nature* **385**, 321–324 (1997).
12. Davis, K. E., Russel, W. B. & Glantschnig, W. J. *Science* **245**, 507–510 (1989).

## The same prion strain causes vCJD and BSE

Epidemiological and clinicopathological studies, allied with pathological prion protein ( $\text{PrP}^{\text{Sc}}$ ) analysis, strongly support the hypothesis that the human prion disease new variant Creutzfeldt–Jakob disease (vCJD) is causally related to bovine spongiform encephalopathy (BSE)<sup>1,2</sup>, but considerable controversy remains. Distinct prion strains are distinguished by their biological properties on transmission to laboratory animals and by physical and chemical differences in  $\text{PrP}^{\text{Sc}}$  strains. We now find that the biological and molecular transmission characteristics of vCJD are consistent with it being the human counterpart of BSE.

We studied transgenic mice expressing only human  $\text{PrP}$  ( $\text{HuPrP}^{\text{Sc}}/\text{Prn-p}^{\text{Sc}}$ ), which have been shown to lack a species barrier to human prions from one iatrogenic CJD case<sup>3</sup>, comparing them with non-transgenic (FVB) mice. All of 16 further CJD cases, encompassing a wide range of clinicopathological phenotypes, all three  $\text{PrP}^{\text{Sc}}$  types reported in sporadic and acquired prion diseases<sup>2</sup> and all *PRNP* genotypes at polymorphic codon 129, a key determinant of genetic susceptibility to human prion diseases<sup>4–6</sup>, were transmitted to these transgenic mice.

Almost all inoculated transgenic mice contracted disease with similar short incubation periods, consistent with a lack of species barrier to these isolates (Table 1). These transgenic mice express human  $\text{PrP}$  homozygous for valine at codon 129. However, there was no significant difference in mean incubation periods between inocula of the different codon 129 genotypes.  $\text{PrP}^{\text{Sc}}$  typing of these transmissions showed that the same prion types seen in sporadic and iatrogenic CJD (types 1–3) are produced, distinct from that seen in vCJD (type 4)<sup>2</sup>. Only occasional transmissions, at longer and variable incubation periods, were seen in FVB mice.

In contrast, efficient transmission of vCJD to FVB mice was observed (Table 1) although incubation periods were prolonged. Conversely, the attack rate of vCJD in the transgenic mice was reduced in comparison to typical CJD, and incubation periods were generally more variable and prolonged. Mean incubation periods to these six vCJD cases were similar in both types of mice. The clinical course in vCJD-inoculated transgenic mice was much longer than in transmissions of typical CJD. vCJD in humans is also associated with a long clinical duration<sup>1</sup>. Some mice, as well as showing typical neurological features, persistently walked backwards. This unusual clinical sign was not seen in transmissions of typical CJD, fatal familial insomnia or other

inherited prion diseases<sup>7</sup>.

BSE transmits efficiently to FVB mice<sup>3</sup>, albeit with prolonged and variable incubation periods (Table 1) which fall to a consistent short incubation period of around 140 days on second passage (data not shown). Transmissions of BSE into the transgenic mice did not occur at incubation periods well beyond those of classical CJD<sup>3</sup>, but we have now observed transmission with much longer incubation periods (Table 1). These transmissions resembled those of vCJD with a long clinical duration and backwards walking in some animals as well as the otherwise typical clinical features of mouse scrapie.

There were striking similarities in PrP deposition patterns between BSE- and vCJD-inoculated animals (detailed neuropathological studies will be published elsewhere). Such patterns are determined by host genotype as well as by agent strain<sup>8</sup>. We saw distinct patterns in the two types of mice, but, in each case, vCJD and BSE produced closely similar patterns. In vCJD- and BSE-inoculated non-transgenic mice, there were PrP plaques and diffuse PrP deposition. In vCJD- and BSE-inoculated HuPrP<sup>+/+</sup> *Prn-p<sup>0</sup>* transgenic mice we saw a predominantly pericellular pattern of PrP immunostaining (data not shown). PrP plaques are a rare feature of prion disease in mice. Occasional mock-inoculated transgenic mice showed weaker and less extensive pericellular PrP immunostaining, probably reflecting the high level of PrP<sup>C</sup> overexpression in these mice. Western blotting for PrP<sup>Sc</sup> was negative in all these controls.

We performed western blot analysis to determine the PrP<sup>Sc</sup> types produced in these transmissions. We have previously shown that the PrP<sup>Sc</sup> type seen in vCJD (type 4) has a ratio of glycoforms closely similar to that of BSE passaged in several other species<sup>2</sup>. vCJD-inoculated FVB mice produced mouse PrP<sup>Sc</sup> with type 4-like glycoform ratios and fragment sizes indistinguishable from those in BSE-inoculated FVB mice (Fig. 1a,b).

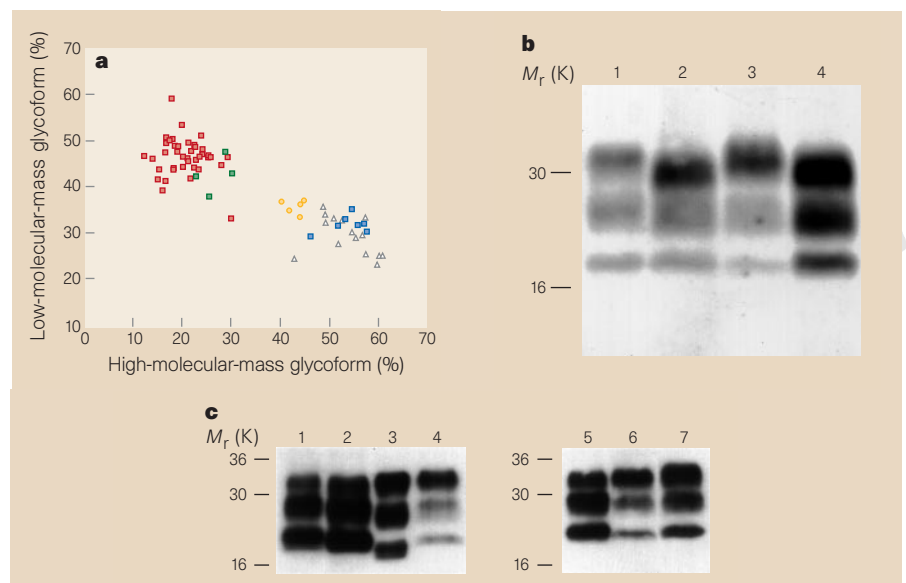


**Figure 1** Transmission of prion diseases to mice. **a**, Scatter graph of proportions of protease-resistant PrP in the high-molecular-mass (di-glycosylated) and low-molecular-mass (mono-glycosylated) glycoforms in individual human cases and FVB mice with experimentally transmitted CJD, vCJD or BSE. Sporadic and iatrogenic CJD cases (PrP<sup>Sc</sup> types 1–3), red squares; vCJD, yellow circles; transmissions of typical CJD to FVB mice, green squares; BSE to FVB mice, blue squares. Transmissions of vCJD to FVB mice, open triangles. **b,c**, Western blots of brain homogenates after pre-treatment with proteinase K using anti-PrP polyclonal antibody 95-108 (ref. 15) (**b**) or anti-PrP monoclonal antibody 3F4 (**c**). Methods were as in ref. 2 except that for PrP glycoform analysis a chemifluorescent substrate (ECF, Amersham) was used and ratios analysed on a Storm 840 Phosphorimager (Molecular Dynamics). **b**, Transmission of vCJD and BSE to non-transgenic (FVB) mice. Lane 1, human vCJD; 2, vCJD-inoculated FVB mouse (same case as lane 1); 3, BSE; 4, BSE-inoculated FVB mouse (same case as in lane 3). **c**, Transmission of vCJD to HuPrP<sup>+/+</sup> *Prn-p<sup>0</sup>* transgenic mice. Lane 1, human CJD, type-2 PrP<sup>Sc</sup>; 2, transgenic mouse inoculated with CJD case from lane 1 showing type-2 pattern; 3, human vCJD case, type-4 PrP<sup>Sc</sup>; 4, transgenic mouse inoculated with vCJD from lane 3 showing type-5 pattern; 5, human CJD case, type-2 PrP<sup>Sc</sup>; 6 and 7, type-5 PrP<sup>Sc</sup> pattern in vCJD-inoculated transgenic mice.

In transmission of vCJD to HuPrP<sup>+/+</sup> *Prn-p<sup>0</sup>* transgenic mice, where human PrP<sup>Sc</sup> is generated, fragment sizes in inoculum and host can be directly compared. Again the PrP<sup>Sc</sup> produced had type 4-like glycoform ratios. However, the fragment sizes differ from those in the inoculum and were indistinguishable from those in the type-2 PrP<sup>Sc</sup> pattern<sup>2</sup> (Fig. 1c). We have designated this new pattern type 5.

A change of fragment size on passage in

mice of a different codon 129 PrP genotype than the inoculum has been reported previously<sup>2</sup>. Type-1 PrP<sup>Sc</sup>, seen in CJD cases of 129MM *PRNP* genotype, consistently converts to type-2 PrP<sup>Sc</sup> on passage in these transgenic mice expressing 129VV human PrP. The glycoform ratios of the original inoculum are also maintained<sup>2</sup>. Abrupt changes in the biological properties ('mutation') of murine scrapie strains on passage in mice of different genotypes are well recognized<sup>9</sup>. We have not, however, been able to show PrP<sup>Sc</sup> by western blotting in BSE-inoculated HuPrP<sup>+/+</sup> *Prn-p<sup>0</sup>* transgenic mice. This may reflect culling of many of these mice soon after clinical diagnosis rather than at a more advanced clinical stage. Though transmission of prion diseases without detectable PrP<sup>Sc</sup> on primary passage has been reported<sup>7,10</sup>, it will be important to confirm transmission by second passage studies.

The prion titres in these primary inocula are unknown but may be higher in the human cases, because cattle with BSE will have been culled before the terminal stages of disease. However, on clinical, pathological and molecular criteria, vCJD shows remarkable similarity in its transmission characteristics to BSE, and is quite distinct from all other forms of sporadic and acquired CJD. These data provide compelling evidence that

Type of inoculum	PRNP codon 129	No. of inocula	Transgenic		Wild type	
			Affected/ inoculated	Incubation period (days)	Affected/ inoculated	Incubation period (days)
spCJD	MM	9	66/67	210 ± 4	0/60	>450 or >600
spCJD	VV	1	5/5	337 ± 11	1/5	471
spCJD	MV	2	15/15	218 ± 2	1/9	257
iCJD (GH)	MM	1	7/7	211 ± 5	1/5	318
iCJD (GH)	MV	1	4/4	195 ± 9	1/5	367
iCJD (GH)	VV	1	5/5	193 ± 4	0/5	>600
iCJD (DM)	MM	1	4/4	204 ± 6	2/4	569, 569
iCJD (G)	VV	1	8/8	187 ± 4	0/5	>600
vCJD	MM	6	25/56	228 ± 15	33/43	371 ± 17
BSE		5	10/26	602 ± 50	21/24	466 ± 26

Incubation periods (mean±s.e.m.) in HuPrP<sup>+/+</sup> *Prn-p<sup>0</sup>* transgenic mice and non-transgenic (FVB) mice. Methods and PRNP analysis were as ref. 2. All CJD cases were neuropathologically confirmed. BSE inocula were pooled brainstem and four individual confirmed cases. Most mice were examined by neuropathology and/or western blotting. Incubation periods are not given for mice that died without definite clinical diagnosis, despite neuropathological or western blot evidence. Numbers affected/inoculated exclude mice dying after inoculation or from intercurrent illness. Controls inoculated with PBS alone did not develop prion disease. spCJD, sporadic CJD; iCJD, iatrogenic CJD; GH, growth hormone; DM, dura mater; G, gonadotrophin; MM, methionine homozygote; MV, methionine/valine heterozygote; VV, valine homozygote.



BSE and vCJD are caused by the same prion strain. Taken together with the temporal and spatial association of vCJD with BSE but not with scrapie or other animal prion diseases, and BSE transmission studies in macaques<sup>11</sup>, this strongly suggests that vCJD is caused by BSE exposure. The theoretical possibility that both BSE and vCJD arise from exposure to a common unidentified source appears remote.

The production of a distinct molecular strain type on transmission of vCJD to mice expressing valine 129 human PrP suggests that BSE transmitted to humans of this genotype might produce a similar strain. Such cases may differ in their clinical and pathological phenotype to vCJD, but could be identified by PrP<sup>Sc</sup> typing.

Although it has been argued that the species barrier resides in PrP primary structure differences between donor and host<sup>12</sup>, our data emphasize that strain type can be as important. As prion propagation involves interactions between PrP<sup>Sc</sup> and host PrP<sup>C</sup>, and strains are associated with differences in PrP conformation and glycosylation<sup>2,13</sup>, such PrP interactions may be most efficient if the interacting proteins are not only of the same sequence but have similar conformational preferences and glycosylation. Mismatch of codon 129 between inoculum and HuPrP<sup>+/+</sup> Prn-p<sup>0/0</sup> mice does not significantly affect CJD transmission, but this could differ for BSE. All vCJD cases have been 129MM genotype (ref. 14 and unpublished data). Although our 129VV mice are much less susceptible to BSE than to typical CJD, suggesting a substantial species barrier, 129MM human PrP mice could be more susceptible.

Andrew F. Hill, Melanie Desbruslais

Susan Joiner, Katie C. L. Sidle

Ian Gowland, John Collinge\*†

Prion Disease Group, Neurogenetics Unit,  
Imperial College School of Medicine at St Mary's,  
London W2 1PG, UK

\*and Department of Neurology, St Mary's Hospital,  
London, W2 1NY, UK

Lawrence J. Doey, Peter Lantos

Department of Neuropathology,  
Institute of Psychiatry, London SE5 8AF, UK

†To whom correspondence should be addressed at the Prion  
Disease Group.

- Will, R. G. *et al. Lancet* **347**, 921–925 (1996).
- Collinge, J., Sidle, K. C. L., Meads, J., Ironside, J. & Hill, A. F. *Nature* **383**, 685–690 (1996).
- Collinge, J. *et al. Nature* **378**, 779–783 (1995); addendum **389**, 526 (1997).
- Baker, H. F. *et al. Lancet* **337**, 1286 (1991).
- Collinge, J., Palmer, M. S. & Dryden, A. J. *Lancet* **337**, 1441–1442 (1991).
- Palmer, M. S., Dryden, A. J., Hughes, J. T. & Collinge, J. *Nature* **352**, 340–342 (1991).
- Collinge, J. *et al. Lancet* **346**, 569–570 (1995).
- Bruce, M. E. *et al. J. Gen. Virol.* **72**, 595–603 (1991).
- Bruce, M. E. *Br. Med. Bull.* **49**, 822–838 (1993).
- Lasmézas, C. I. *et al. Science* **275**, 402–405 (1997).
- Lasmézas, C. I. *et al. Nature* **381**, 743–744 (1996).
- Prusiner, S. B. *et al. Cell* **63**, 673–686 (1990).
- Telling, G. C. *et al. Science* **274**, 2079–2082 (1996).
- Collinge, J. *et al. Lancet* **348**, 56 (1996).
- Piccardo, P. *et al. J. Neuropathol. Exp. Neurol.* **56**, 589 (1997).

## 'Male-stuffing' in wasp societies

Intracolony aggression within and between castes of social insects is common<sup>1–3</sup>. We have observed an unusual aggressive interaction between nestmates of the paper wasp *Polistes dominulus*. In response to foragers returning to the colony, females (workers) initiate aggressive encounters with males culminating with the male being forced head-first into an empty nest-cell ('male-stuffing'). 'Stuffed' males are unable to feed, so the behaviour seems to ensure that food is preferentially channelled to larvae, which are likely to be more closely related to the workers than are the adult males.

We observed two categories of stuffing. 'Initial stuffing' (Fig. 1) began with antenna-to-antenna contact and was followed by grappling, biting, and sting-threats. The aggressor then forced the recipient head-first into an empty cell. 'Repeated stuffing' was characterized by biting and pushing the abdomen of an individual whose head and thorax were already inside a cell.

We studied the behaviour by transcribing and analysing 26 hours of videotape. We saw stuffing behaviour only in colonies containing males ( $n=5$  colonies) and not in those without ( $n=6$  colonies; sexed by antennal morphology<sup>2</sup>;  $\chi^2=21$ ,  $P<0.001$ ). Stuffing was directed exclusively at males, despite their being greatly outnumbered by females (1:4.21) in colonies of both sexes (binomial test,  $P<0.0001$ ). Of 66 stuffing events, 46 were directed at males from that colony (identified by marking them at eclosion); the remainder were of unknown origin. Queens ( $n=5$ ) did not stuff males (0/66 events; binomial test,  $P<0.1$ ). All stuffing was done by workers other than the returning forager.

Initial stuffing occurred soon after the return of a forager, whereas repeated stuff-

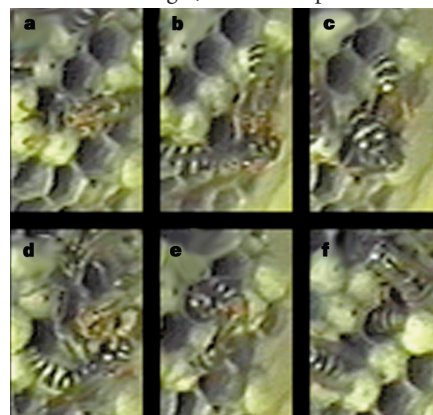


**Figure 1** Initial male-stuffing. **a**, Male on the comb. **b**, Female (worker) approaches and antennates him, **c**, followed by biting and sting-threats. **d**, She stuffs him into an empty cell, **e**, and pushes on his abdomen. **f**, Male in the cell.

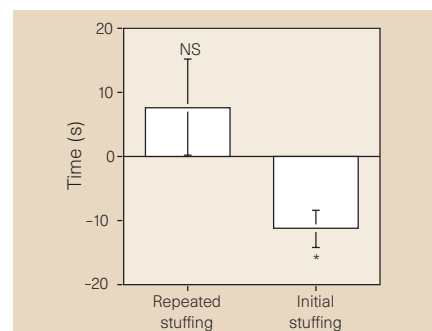


**Figure 2** Difference between the time from most recent male arrival until stuffing and half the average interval between returns. A value of 0 is expected if male-stuffing is random with respect to arrivals. Initial stuffing ( $n=32$ ) occurred shortly after a nestmate returned ( $\bar{t}=18.86 \pm 2.89$  s; Wilcoxon signed-rank test:  $Z=-3.20$ ,  $*P<0.01$ ), but repeated stuffing ( $n=34$ ) occurred randomly with respect to arrivals ( $\bar{t}=39.88 \pm 7.51$  s;  $Z=-0.18$ ,  $P>0.8$ ; NS). Means  $\pm$  s.e.m.

ing occurred at random times (Fig. 2). Males that had been repeatedly stuffed remained in cells 6.35 times longer ( $\bar{t}=384.29 \pm 43.01$  s; mean time  $\pm$  s.e.m.) than the mean time between forager arrivals ( $\bar{t}=60.53 \pm 2.25$  s;  $n=833$ ). Thus, stuffing may function to preclude males from gaining access to resources gathered by the workers.

Limiting food consumption by males may maximize the inclusive fitness of workers, who should direct their help towards closely related kin<sup>4,5</sup>. Feeding future reproductive females provides a larger fitness pay-off than feeding adult males<sup>6</sup>. Workers from a colony containing one singly mated queen have a relatedness to sisters of 0.75. Workers are only related by 0.25 to brothers, 0.375 to nephews (worker-produced males) and are unrelated to immigrant males.

Assuming that female larvae are present, workers are more closely related to reproductive-destined larvae than to adult males. Even in circumstances where workers are, on average, equally related to male and female nestmates (such as brothers and half-sisters when the queen has mated more than once), feeding needy larvae may provide a larger inclusive fitness pay-off than feeding adult males, which can forage for themselves. Preferential channelling of resources to larvae, by stuffing males, may maximize the genetic self-interest of worker wasps.

Philip T. Starks, Emily S. Poe

Section of Neurobiology and Behavior,  
W311 Seeley G. Mudd Hall, Cornell University,  
Ithaca, New York 14853-2702, USA  
e-mail: pts3@cornell.edu

- Ratnieks, F. L. W. Thesis, Cornell Univ., Ithaca (1989).
- Reeve, H. K. in *The Social Biology of Wasps* (eds Ross, K. G. & Matthews, R. H.) 99–148 (Cornell Univ. Press., Ithaca., 1991).
- Gamboja, G. J. in *Natural History and Evolution of Paper-Wasps* (eds Turillazzi, S. & West-Eberhard, M. J.) 161–177 (Oxford Univ. Press., 1996).
- Hamilton, W. D. *J. Theor. Biol.* **7**, 1–16 (1964).
- Hamilton, W. D. *J. Theor. Biol.* **7**, 17–52 (1964).
- Hamilton, W. D. *Annu. Rev. Ecol. Systemat.* **3**, 193–232 (1972).